

Temperature Dependence of the Isotropic Hyperfine Coupling Constants in 1,4-Hydroquinone and 1,4-Dihydroxynaphthalene Cation Radicals

Jussi Eloranta* and Mikko Vuolle

Department of Chemistry, University of Jyväskylä, P.O. Box 35, FIN-40351 Jyväskylä, Finland

Received 16 June 1997; revised 5 September 1997; accepted 9 September 1997

ABSTRACT: The temperature dependences of hydroxyl group proton and ring proton isotropic hyperfine coupling constants (IHFC) of 1,4-hydroquinone (HQ) and 1,4-dihydroxynaphthalene (NQ) cation radicals were measured by electron paramagnetic resonance spectroscopy. The spectral parameters were obtained in the temperature range 150–300 K using various solvents. The hydroxyl group proton IHFC data obtained were fitted to the theoretical temperature dependence model, yielding the hydroxyl group rotation barrier height and completely planar hydroxyl proton IHFC value. Experimental results are discussed with reference to theoretical density functional calculations. The new experimental rotation barrier heights for HQ and NQ cation radicals are 59 ± 4 and 37 ± 4 kJ mol⁻¹ in nitromethane, respectively. © 1998 John Wiley & Sons, Ltd.

KEYWORDS: isotropic hyperfine coupling constants; 1,4-hydroquinone cation radical; 1,4-dihydroxynaphthalene cation radical; temperature dependence; rotation barrier; electron paramagnetic resonance spectroscopy

INTRODUCTION

The radical cations of 1,4-hydroquinone (HQ) and 1,4-dihydroxynaphthalene (NQ) may be produced in strongly acidic media with suitable oxidants.^{1,2} These compounds exist in doubly protonated form under these conditions.³

The internal barriers to rotation of the hydroxyl groups in HQ and NQ cation radicals have been determined earlier experimentally as 42 ± 8 and 25 ± 6 kJ mol⁻¹, respectively, in the liquid phase.⁴ The calculated theoretical rotation barrier height for HQ cation radical in the gas phase is slightly higher than the experimental value, 46 kJ mol⁻¹.⁵ This high rotation barrier causes *cis-trans* isomerism in the HQ cation radical, which has been detected experimentally at 230 K by electron paramagnetic resonance (EPR) and ENDOR spectroscopy.^{1,2,4,6}

The EPR spectra of HQ and NQ cation radicals exhibit temperature-dependent behaviour, temperature dependence of isotropic hyperfine coupling constants (IHFCs) and linewidth alternation. These effects have been investigated earlier by Sullivan and co-workers.^{4,6} The temperature dependence of the hydroxyl proton IHFC was assigned as originating from the torsional oscillations of this group at the bottom of a deep potential well.^{4,5} The zero point and temperature-dependent correction for this IHFC was calculated earlier by Eloranta *et al.*⁵ The ratio for the protonated and deuterated hydroxyl group IHFCs, a_H/a_D , was observed to be

generally higher than predicted by the ratio of the magnetogyric ratios. This is caused by the change in the reduced moment of inertia of the rotating groups.^{1,5}

The IHFCs for the *cis* and *trans* isomers of HQ cation radical have been measured experimentally by Vuolle *et al.*¹ using ENDOR spectroscopy. Identification of the *cis* and *trans* isomers has been proposed earlier by Sullivan.⁶ IHFCs for NQ cation radical have been measured by Sullivan⁴ and Bolton *et al.*³ Assignment of the IHFCs to specific positions in both radicals was proposed by Barabas *et al.*⁶

In this study, we applied the method originally described by Bauld *et al.*⁷ to model the temperature-dependent effects of the IHFCs in the HQ and NQ cation radicals. A similar method for these compounds was applied earlier by Sullivan.⁴ For determination of the experimental rotation barrier heights, this work was essentially a re-examination of Sullivan's work. In contrast to his study, the method is enhanced by accurate numerical solution of the one-dimensional torsional Schrödinger equation, least-squares fitting, high-accuracy EPR simulations and density functional (DFT)-based IHFC and energy calculations. A larger temperature scale was also achieved by a careful choice of solvent. Finally, the experimental results were compared with data calculated by the theoretical DFT method.

EXPERIMENTAL

Materials

The cation radicals were produced from neutral HQ (fotopur) from Merck and 1,4-naphthoquinone (puriss.) from Fluka. Other chemicals used were fluorosulfonic

* Correspondence to: J. Eloranta, Department of Chemistry, University of Jyväskylä, P.O. Box 35, FIN-40351 Jyväskylä, Finland.
E-mail: eloranta@jyu.fi

acid (FSA) (triply distilled) from Aldrich, deuterated sulfuric acid (DSA, 96–98% D) from Merck, nitromethane (NM) (purum) from Fluka and sulfuryl chloride fluoride (SCF) (distilled, 99%) from Acros Organics.

Equipment and Sample Preparation

EPR spectra were measured on a Bruker ESP-300 spectrometer with 12.5 or 100 kHz modulation frequency and modulation amplitude $< 2 \mu\text{T}$. The applied microwave power for all samples was $\leq 0.5 \text{ mW}$ to avoid power saturation. Accuracy of the temperature controller was enhanced by a calibration curve, and the estimated maximum error was $\pm 2 \text{ K}$.

The quinone was inserted in the sample cuvette and FSA or DSA was added. The resulting solution was mixed thoroughly and the solvent, NM or SCF (distilled under vacuum), was added. The amount of FSA or DSA was kept to the minimum (*ca.* 10%) in order to obtain maximum resolution for the spectrum. The solution was then frozen in liquid nitrogen and connected to the vacuum line [*ca.* 10^{-7} Torr (1 Torr = 133.3 Pa)]. After two freeze–pump–thaw cycles, the cuvette was sealed with a flame. The resulting sample radical concentration was *ca.* 10^{-4} – $10^{-3} \text{ mol dm}^{-3}$.

Simulation of EPR Spectra

The root-mean-square (RMS) error between the experimental and first-order simulated EPR spectra was minimized by the Monte Carlo and simplex procedures provided in the xemr package.^{8,9} Given a suitable initial guess of the spectral parameters, this process yields estimates for the variables with good accuracy. The ENDOR derived IHFC values were used as initial guess data.¹ In the case of HQ cation radical the simulation consisted of two spectra, for the *cis* and *trans* isomers, which were summed before the RMS error was calculated. The optimization initially contained restrictions among the spectral parameters of the isomers in order to avoid convergence to a local minimum. The isotropic first-order simulation procedure included the nuclear spin dependent linewidth alternation which is caused by the introduction of the anisotropic effects to the spectrum.¹⁰ Degenerate EPR transitions were assumed to consist of a single Lorentzian line.¹¹ For studies of the linewidth alternations, the well known four-jump model was applied. The average lifetimes of the conformations were calculated by using the Norris equation as implemented in the xemr program.^{8,12} The average lifetime was included in the set of optimized parameters.

Hydroxyl Group Temperature Dependence

The temperature dependence model of the hydroxyl protons in the HQ cation radical has been presented earlier.⁵ This procedure was also applicable to the NQ cation radical, as will be justified in the Discussion section. If the IHFC barrier height is chosen to be con-

stant, then the experimental hydroxyl proton temperature dependence may be used to obtain estimates for a_p and V_0 , where a_p denotes the completely planar hydroxyl proton IHFC and V_0 the hydroxyl group rotation barrier height. The applied IHFC barrier heights were obtained from the DFT calculations as described later. The torsional dependences of IHFC and potential energy were described by one Fourier term. The least-squares method was used in fitting the experimental data to the theoretical model.⁵ Since the torsional Schrödinger equation was solved, the procedure also yielded the zero-point energy correction due to torsional oscillation.

The initial guess for the variables must be reasonable in order to avoid convergence to a local minimum in the least-squares fit. Solution of the one-dimensional torsional Schrödinger equation depends on the reduced moment of inertia of the rotating groups, and therefore deuteration of the hydroxyl group offers a suitable method for revalidating the results. The error ranges for the rotation barriers were derived from the estimated errors in the IHFC barrier height. Routines of the Numerical Algorithms Group (NAG) Library MK16 were used in the calculations.¹³

Density Functional Calculations

The optimum *cis*, *trans* and transition state (TS) geometries of the HQ cation radical were obtained from earlier calculations.¹⁴ Corresponding geometries for NQ cation radical were calculated by the UB3LYP/6–31G* DFT method.¹⁵ The UB3LYP method is the spin unrestricted Becke's three-parameter hybrid method with the Lee–Yang–Parr correlation functional.^{16–19} The TS geometry was calculated by constraining the hydroxyl group proton torsion angle to be completely out of the quinone ring plane and by performing a constrained geometry optimization. The correct number of imaginary frequencies was verified for each optimized structure by separate single-point frequency runs. All the calculated molecules were cation radicals having an electronic doublet state.

The NQ cation radical may exist in two different planar *cis* forms and in one planar *trans* form. The *cis* 1 form has both hydroxyl protons pointing away from the protons at positions 5 and 8. Correspondingly, the *cis* 2 form has the hydroxyl protons pointing towards positions 5 and 8.

The IHFC values were calculated from the normalized spin densities at the magnetic nuclei as described elsewhere.²⁰ All the DFT calculations were performed by the Gaussian 94 program on Digital Alpha and Cray C94 computers.²¹

RESULTS

HQ Cation Radical

The experimental spectral parameters for HQ cation radical in NM–FSA, NM–DSA and SCF–FSA at 230 K

Table 1. Experimental spectral parameters at 230 K for HQ cation radical obtained from the EPR simulations^a

Solvent	Conformation	a_1 ($2 \times$)	a_2 ($2 \times$)	a_3 ($2 \times$)	Linewidth	Ratio (%)
NM-10% FSA	<i>trans</i>	0.3329	0.2066	0.2468	3.33	51
	<i>cis</i>	0.3262	0.2371	0.2156	3.27	49
NM-10% DSA	<i>trans</i>	0.0530	0.2076	0.2448	5.30	50
	<i>cis</i>	0.0530	0.2373	0.2152	5.93	50
SCF-10% FSA	<i>trans</i>	0.3487	0.2022	0.2513	3.92	50
	<i>cis</i>	0.3484	0.2396	0.2135	4.13	50

^a IHFC values (a_i) are expressed in mT and linewidths in μ T. The ratio column represents the ratio of signal intensities for the two isomers.

are given in Table 1. Corresponding temperature dependence data for the IHFCs are shown in Fig. 1. The temperature dependences predicted by the theoretical model are also shown by continuous lines using the values in Table 2.

The least-squares fit derived rotation barrier heights, completely planar hydroxyl proton IHFCs and the tor-

sional zero-point energies for the solvents used are listed in Table 2. Estimated errors for the rotation barriers were ± 4 kJ mol⁻¹.

HQ cation radical samples in 10, 40 and 50% FSA in NM were prepared in order to investigate the effect of the acid concentration on the hydroxyl group proton temperature dependence. The acid concentration did not change the shape of the temperature dependence curve but introduced only a constant change, as can be seen in Fig. 1.

The linewidth alternation in SCF-FSA in the high-temperature region is shown in Fig. 2. The activation energy was extracted from an Arrhenius plot ($\ln k$ vs. $1/T$) obtained by the least-squares fitting. The rotation barrier obtained by this method was 50.3 ± 4 kJ mol⁻¹. The error range was obtained directly from the least-squares fit.

Table 2. Experimental rotation barriers (kJ mol⁻¹), completely planar hydroxyl proton IHFCs (mT) and torsional zero point energies (kJ mol⁻¹) for HQ cation radical in various solvents

Solvent	Rotation barrier	Planar IHFC	Zero point energy
NM-10% FSA	59.4	-0.428	3.8
NM-40% FSA	59.1	-0.430	3.7
NM-50% FSA	58.8	-0.431	3.7
NM-10% DSA	68.4	-0.414	2.9
SCF-10% FSA	52.7	-0.451	3.5
SCF-15% FSA	52.5	-0.451	3.5

NQ Cation Radical

Table 3 lists the spectral parameters for NQ cation radical in NM-FSA, NM-DSA and SCF-FSA at 230

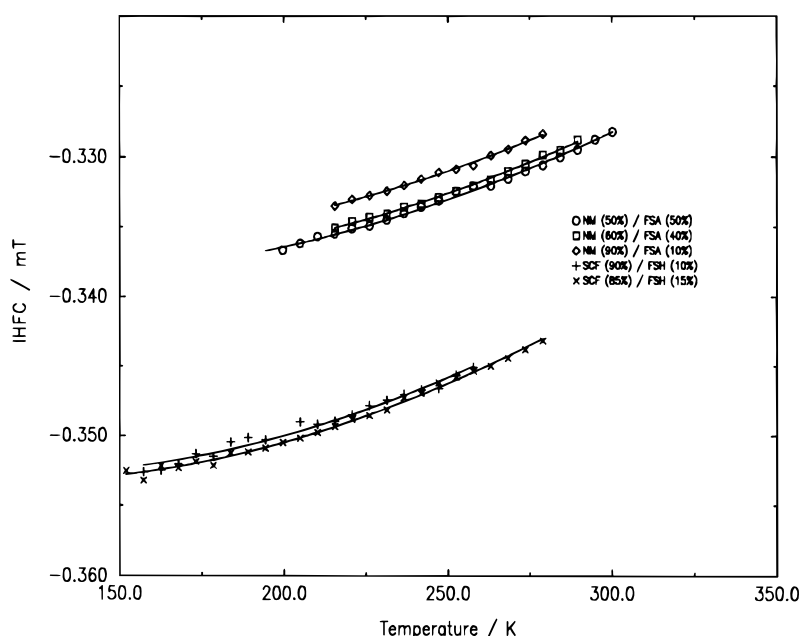
**Figure 1.** Temperature dependence of the hydroxyl proton IHFC in HQ cation radical. The continuous lines were obtained from least-squares fitting to the theoretical model.

Table 3. Experimental spectral parameters for NO cation radical at 230 K^a

Solvent	a_1 (2 ×)	a_2 (2 ×)	a_3 (2 ×)	a_4 (2 ×)	Linewidth
NM-10% FSA (<i>cis</i> 1)	0.2416	0.3074	0.1663	0.0819	9.31
NM-10% DSA (<i>cis</i> 1)	0.0387	0.3076	0.1600	0.0821	4.24
SCF-10% FSA (<i>cis</i> 1)	0.2461	0.3105	0.1808	0.0836	6.11

^a IHFC values are expressed in mT and linewidths in μ T.

K. The obtained hydroxyl group rotation barrier heights, completely planar hydroxyl proton IHFCs and torsional zero point energies are given in Table 4. The estimated errors for rotation barriers were ± 4 kJ mol⁻¹. Only one isomer was detected throughout the applied temperature range.

DFT Calculations

The DFT calculated IHFC values, energy differences and Boltzmann populations at 230 K for HQ^{5,14} and NQ cation radicals are listed in Table 5. The zero-point

Table 4. Experimental rotation barriers (kJ mol⁻¹), completely planar hydroxyl proton IHFCs (mT) and torsional zero point energies (kJ mol⁻¹) for NQ cation radical in various solvents

Solvent	Rotation barrier	Planar IHFC	Zero point energy
NM-10% FSA	36.7	-0.336	3.0
NM-10% DSA	40.3	-0.323	2.2
SCF-10% FSA	35.7	-0.341	2.9

energy corrections lowered the rotation barrier height by *ca.* 5 kJ mol⁻¹ in both HQ and NQ cation radicals.

The expectation values of the S^2 operator were < 0.76 and exactly 0.75 after the annihilation of the higher states for all the DFT calculations.

DISCUSSION

Hydroxyl Group Rotation Barriers

The obtained hydroxyl group rotation barrier in HQ cation radical was higher than that reported by Sullivan and co-workers.^{4,6} The barrier was *ca.* 30% higher than the theoretical value in the gas phase. The deuterated sample showed a slightly higher rotation barrier than the non-deuterated species but was still of the same order of magnitude. The values obtained compared favorably with the approximate barrier height obtained from the Arrhenius plot. The SCF-FSA solvent system produced the lowest rotation barrier and the completely planar hydroxyl proton IHFC closest to the DFT calculated value. This means that there was only a weak interaction between the solvent and the radical molecule. The lowered rotation barrier permitted the detec-

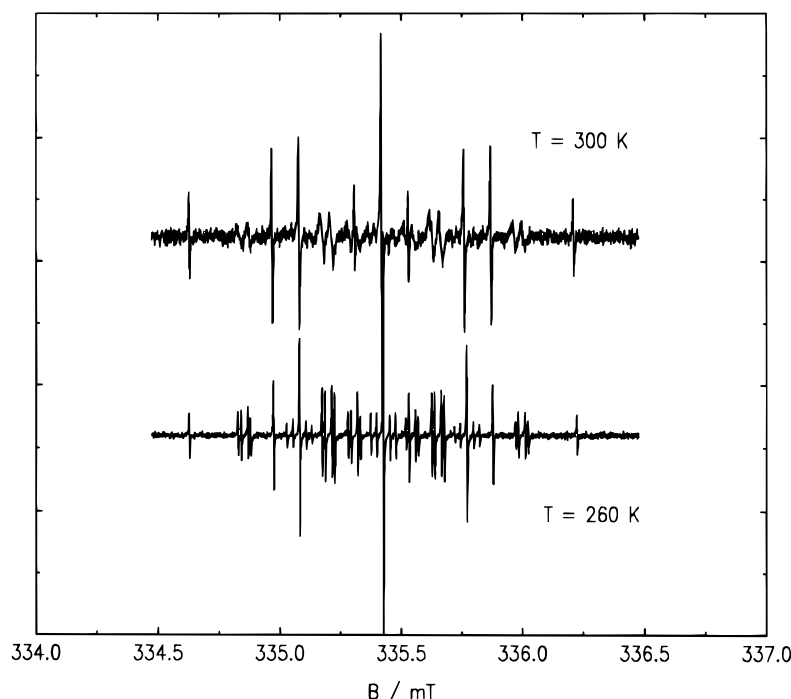
**Figure 2.** Temperature dependent linewidth alternation in HQ cation radical (SCF-FSA).

Table 5. IHFC values (mT) for *cis*, *trans* and TS conformations of HQ^{5,14} and NQ cation radicals computed by the UB3LYP/6–31G* DFT method^a

Cation radical	conformation	a_{OH} (1)	a_{OH} (4)	a_2	a_3	a_5	a_6	ΔE	Ratio (%)		
HQ	<i>cis</i>	−0.459	−0.459	−0.176	−0.176	−0.241	−0.241	1.2	35		
	<i>trans</i>	−0.462	−0.462	−0.271	−0.148	−0.271	−0.148	0.0	65		
	TS	+2.40	−0.503	−0.117	−0.293	−0.362	−0.012	46	0		
		a_{OH} (1)	a_{OH} (4)	a_2	a_3	a_5	a_6	a_7	a_8	ΔE	Ratio (%)
NQ	<i>cis</i> 1	−0.298	−0.298	−0.325	−0.325	−0.274	−0.078	−0.077	−0.274	0.0	98
	<i>cis</i> 2	−0.351	−0.351	−0.256	−0.257	−0.212	−0.081	−0.081	−0.212	17	0
	<i>trans</i>	−0.350	−0.307	−0.347	−0.239	−0.216	−0.115	−0.042	−0.259	7.2	2
	TS	+1.75	−0.288	−0.178	−0.359	−0.296	−0.171	−0.024	−0.404	35	0

^a The energy differences (kJ mol^{−1}) and Boltzmann populations are indicated for each structure. Energies include the zero point energy corrections.

tion of the linewidth alternation effects in HQ cation radical in the high-temperature region.

In the case of NQ cation radical three isomers exist which differ in energy and IHFCs. Before the temperature dependence model could be applied the results of theoretical DFT calculations were inspected. The calculations showed that there was only one dominant isomer (*cis* 1). The IHFC barrier height was obtained with respect to this conformation and the closest TS. This allowed the use of the temperature dependence model. The barrier heights obtained were about 17 kJ mol^{−1} smaller than in HQ. The rotation barrier was only slightly higher than was predicted by the theoretical gas-phase calculations and was therefore unexpectedly small. Deuterated samples produced approximately the same rotation barriers as the undeuterated species.

In general, the rotation barrier heights were about 40% larger than the earlier values reported by Sullivan and co-workers.^{4,6} The reason for this difference appeared to be the too small estimate of the IHFC barrier height in Sullivan and co-workers' work. In the case of HQ cation radical, the rotation barrier height from the hydroxyl proton IHFC temperature dependence model with the new corrected IHFC barrier height is in agreement with the results obtained from exchange simulations and theoretical calculations.^{5,14}

Identification of Isomers

Identification of the isomers in HQ cation radical (Table 1) was achieved from the small intensity differences in the EPR simulations (NM-FSA) and comparison of the experimental IHFC magnitudes with the theoretically calculated values. This assignment is the same as the earlier McLachlan perturbed Hückel-based proposition made by Barabas *et al.*⁶ The reason for the differences between the calculated ring proton IHFCs and the experimental IHFCs was probably due to solvent effects.⁵ After the *cis*–*trans* isomers had been identified, the assignment of IHFCs to specific positions may be performed by inspection of the data in Tables 1

and 5. Solvation caused a strong stabilization of the *cis* isomer since the isomer ratio is almost 50:50 as compared with the theoretically calculated Boltzmann populations (35:65) in the gas phase.

Since the NQ hydroxyl group proton IHFCs were the same, then only the two planar *cis* forms (*cis* 1 and *cis* 2) could be occurring. According to the theoretical calculations, the *cis* 2 conformation is considerably higher in energy than *cis* 1. Only one isomer was detected in the NQ cation radical samples. Therefore, we assigned the species present as *cis* 1. The theoretically calculated IHFCs for *cis* 1 were in reasonable agreement with the observed IHFCs (Tables 3 and 5). The largest deviation was at positions 5 and 8, where the difference is large, *ca.* 0.1 mT.

General Remarks

The IHFC rotation barrier must be known if only the linear part of the IHFC *vs.* temperature curve is available. In this work we were only able to reach a small part of the non-linear section and therefore we did not feel confident in varying the IHFC barrier height in the least-squares fitting. The current DFT based methods can be of great help in obtaining the approximate IHFC barrier height. Also, in this work we assumed that the IHFC barrier height was not a function of the solvent. The motivation for this approximation can be seen from the data in Fig. 1. The largest source of error is the IHFC barrier height, and the error analysis may be based on the estimated error in it. We expected that the applied DFT model calculated the hydroxyl proton IHFC with an accuracy of 10–15%. This observation was based on our calculation of IHFCs in a series of small organic radicals.

The iterative simulations of the EPR spectra had many parameters to be optimized. It was essential that as many parameters as possible were obtained from the spectra manually and kept constant. It was also important to inspect the plots of the multipliers of the nuclear spin dependent linewidth parameters. The 'continuous'

behaviour of the spectral parameters against temperature gives a good criterion for correctness of the simulations.

CONCLUSIONS

The temperature dependence of the hydroxyl group proton IHFC can be used to estimate the rotation barrier height and the completely planar hydroxyl proton IHFC value in cases where the IHFC difference between the ground and the transition states is large. The liquid-phase rotation barrier of HQ cation radical was of the correct magnitude when compared with the theoretically calculated gas-phase barriers. The earlier determinations of rotation barriers in these compounds gave too low values because the estimated IHFC barrier height was too small.

REFERENCES

1. M. Vuolle, R. Mäkelä and J. A. Eloranta, *J. Chem. Soc. Faraday Trans.* **88**, 2173 (1992).
2. W. F. Forbes and P. D. Sullivan, *J. Am. Chem. Soc.* **88**, 2862 (1966).
3. J. R. Bolton, A. Carrington and J. dos Santos-Veiga, *Mol. Phys.* **5**, 465 (1962).
4. P. D. Sullivan, *J. Phys. Chem.* **75**, 2195 (1971).
5. J. Eloranta, R. Suontamo and M. Vuolle, *J. Chem. Soc., Faraday Trans.* **93**, 3313 (1997).
6. A. B. Barabas, W. F. Forbes and P. D. Sullivan, *Can. J. Chem.* **45**, 267 (1967).
7. N. L. Bauld, J. D. McDermid, C. E. Hudson, Y. S. Rim, J. Zoeller, Jr., R. D. Gordon and J. Hyde, *J. Am. Chem. Soc.* **91**, 6666 (1969).
8. J. Eloranta, <ftp://endor.chem.jyu.fi/pub>.
9. B. Kirste, *Anal. Chim. Acta* **265**, 191 (1992).
10. G. K. Fraenkel, *J. Phys. Chem.* **71**, 139 (1967).
11. J. H. Freed and G. K. Fraenkel, *J. Chem. Phys.* **39**, 326 (1963).
12. J. R. Norris, Jr, *Chem. Phys. Lett.* **1**, 333 (1967).
13. Numerical Algorithms Group (NAG) Library MK16, Oxford (1993).
14. J. Eloranta, V. Vatanen, K. Vaskonen, R. Suontamo and M. Vuolle, *J. Mol. Struct. (Theochem)*, in press.
15. M. S. Gordon, *Chem. Phys. Lett.* **76**, 163 (1980).
16. A. D. Becke, *J. Chem. Phys.* **98**, 5648 (1993).
17. S. H. Vosko, L. Wilk and M. Nusair, *Can. J. Phys.* **58**, 1200 (1980).
18. C. Lee, W. Yang and R. G. Parr, *Phys. Rev. B* **37**, 785 (1988).
19. B. Miehlich, A. Savin, H. Stoll and H. Preuss, *Chem. Phys. Lett.* **157**, 200 (1989).
20. R. McWeeny, *Methods of Molecular Quantum Mechanics*, 2nd ed. Academic Press, London (1992).
21. M. J. Frisch, G. W. Trucks, H. B. Schlegel, P. M. W. Gill, B. G. Johnson, M. A. Robb, J. R. Cheeseman, T. A. Keith, G. A. Petersson, J. A. Montgomery, K. Raghavachari, M. A. Al-Laham, V. G. Zakrzewski, J. W. Ortiz, J. B. Foresman, J. Cioslowski, B. B. Stefanov, A. Nanayakkara, M. Challacombe, C. Y. Peng, P. Y. Ayala, W. Chen, M. W. Wong, J. L. Anders, E. S. Replogle, R. Gomperts, R. L. Martin, D. J. Fox, J. S. Binkley, D. J. Defrees, J. Baker, J. P. Stewart, M. Head-Gordon, C. Gonzalez and J. A. Pople, *Gaussian 94 Revision B.3*. Gaussian, Pittsburgh, PA (1995).